Available online at www.sciencedirect.com
SCIENCE DIRECT
International Journal of Pharmaceutics 308 (2006) 160–167
INTERNATIONAL JOURNAL OF PHARMACEUTICS
www.elsevier.com/locate/ijpharm

# Combination of adsorption by porous $CaCO_3$ microparticles and encapsulation by polyelectrolyte multilayer films for sustained drug delivery

Chaoyang Wang, Chengyi He, Zhen Tong*, Xinxing Liu, Biye Ren, Fang Zeng

*Research Institute of Materials Science, South China University of Technology, Guangzhou 510640, China*

Received 16 September 2005; received in revised form 26 October 2005; accepted 5 November 2005
Available online 15 December 2005

**Abstract**

Combination of adsorption by porous $CaCO_3$ microparticles and encapsulation by polyelectrolyte multilayers via the layer-by-layer (LbL) self-assembly was proposed for sustained drug release. Firstly, porous calcium carbonate microparticles with an average diameter of 5 μm were prepared for loading a model drug, ibuprofen (IBU). Adsorption of IBU into the pores was characterized by ultraviolet (UV), infrared (IR), thermogravimetric analysis (TGA), Brunauer–Emmett–Teller (BET) experiment and X-ray diffraction (XRD). The adsorbed IBU amount $\Gamma$ was 45.1 mg/g for one-time adsorption and increased with increasing adsorption times. Finally, multilayer films of protamine sulfate (PRO) and sodium poly(styrene sulfonate) (PSS) were formed on the IBU-loaded $CaCO_3$ microparticles by the layer-by-layer self-assembly. Amorphous IBU loaded in the pores of the $CaCO_3$ microparticles had a rapider release in the gastric fluid and a slower release in the intestinal fluid, compared with the bare IBU crystals. Polyelectrolyte multilayers assembled on the drug-loaded particles by the LbL reduced the release rate in both fluids. In this work, polymer/inorganic hybrid core-shell microcapsules were fabricated for controlled release of poorly water-soluble drugs. The porous inorganic particles are useful to load drugs in amorphous state and the polyelectrolyte multilayer films coated on the particle assuage the initial burst release.


*Keywords:* Porous $CaCO_3$; Layer-by-layer; Polyelectrolyte multilayer films; Encapsulation

## 1. Introduction

Various drug delivery systems, such as liposomes, micelles, emulsions, polymeric micro/nanoparticles etc., have been showing great promise in controlled and targeted drug delivery (Benita, 1996; Allen and Cullis, 2004; Brigger et al., 2002; Torchilin, 2005). These techniques are capable of controlling the rate and duration of drug delivery and/or targeting the drug to the specified cell or tissue. Recently, porous inorganic materials are emerging as a new category of host/guest drug delivery systems due to some interesting features of biological stability and controlled release property. These materials possess vast amounts of nanopores that allow the inclusion of drugs in them. Several porous minerals have been used including synthetic zeolite (Fisher et al., 2003), silica xerogel materials (Suzuki et al., 2001; Kortesuo et al., 2001; Otsuka et al., 2000; Charnay et al., 2004), porous hollow silica nanoparticle (Li et al., 2004), porous hydroxyapatite (Kim et al., 2004), porous silica–calcium phosphate composite (El-Ghannam et al., 2005), porous calcium carbonate microparticle (Volodkin et al., 2004a,b) and other porous ceramics. Some novel controlled release carriers have been developed. Suzuki et al. (2001) reported a thermo-responsive silica-poly(*N*-isopropylacrylamide) hybrid gel as a carrier of Brilliant Blue F for controlled drug delivery. Kortesuo et al. (2001) have used porous silica xerogel to entrap dexmedetomidine, and have evaluated the release rate from the matrix. Otsuka et al. (2000) investigated the surface-modification of silica gel with the silane coupling to improve the surface affinity to an oily medicine, phytonadione. However, a rapid release during the whole process, especially an initial burst release has been observed in some cases when inorganic porous particles were used as the drug host. Charnay et al. (2004) reported that the ibuprofen (IBU) was nearly completely released only during the initial 60 min from porous silica material, MCM 41. Li et al. (2004) found that about 70% Brilliant Blue F was released during the initial burst release from the porous silica nanoparticles.

* Corresponding author. Tel.: +86 20 87112886; fax: +86 20 87112886.
*E-mail address:* mcztong@scut.edu.cn (Z. Tong).

0378-5173/$ – see front matter © 2005 Elsevier B.V. All rights reserved.
doi:10.1016/j.ijpharm.2005.11.004

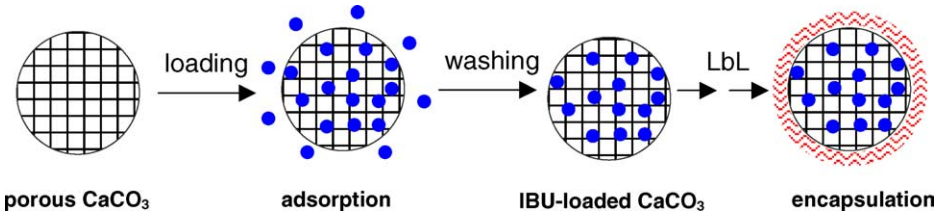


Fig. 1. Schematic representation for combination of adsorption by porous $CaCO_3$ microparticles and encapsulation by polyelectrolyte multilayer films for drug release.

One possibility for reducing the release rate and suppressing the initial burst is encapsulating the drug-loaded particles with thin polymeric films.

Layer-by-layer (LbL) self-assembly technique has been a powerful tool for the micro-encapsulation (Caruso, 2001; Peyratout and Dahne, 2004; Decher and Schlenoff, 2003), where polyelectrolyte multilayer films were elaborated on various particles through alternating deposition of oppositely charged polyelectrolytes mainly due to the electrostatic attraction (Sun et al., 2005). This micro-encapsulation via LbL showed potential applications in biochemistry, pharmacy, controlled release, cosmetic and catalyst by several approaches (Decher and Schlenoff, 2003; Liang et al., 2004). The first approach was directly using proteins, e.g., bovine serum albumin (BSA) (Caruso and Möhwald, 1999), glucose oxidase (GOD) (Schuler and Caruso, 2000), urease (Liang et al., 2005) and superoxide dismutase (SOD) (He et al., 2005), as the depositing species to prepare bioactive core-shell particles. The second approach was directly coating drug microcrystals, such as ibuprofen (Qiu et al., 2001; An et al., 2004), furosemide (Ai et al., 2003), Vitamin $K_3$, insulin (Dai et al., 2004), dexamethasone (Pargaonkar et al., 2005; Zahr et al., 2005) and indomethacin (Ye et al., 2005a) with polyelectrolyte multilayer films for prolonged release. The third method was removal of the template particles to fabricate hollow polyelectrolyte multilayer capsules and drugs, enzymes, or other biomacromolecules were loaded into these hollow capsules for the delivery (Mao et al., 2005; Tiourina and Sukhorukov, 2002; Ye et al., 2005b). Another method is encapsulating the drug/organic or inorganic composites hybrid particles with polyelectrolyte multilayer films to control the release.

In this work, we have proposed a new combination method for sustained drug release of adsorption by porous $CaCO_3$ microparticles and encapsulation of the drug-loaded microparticles with polyelectrolyte multilayer films formed by the LbL self-assembly. Fig. 1 illustrates the fabricating procedure of this novel drug delivery system. IBU was selected as a model drug since its properties were well documented and widely used as an anti-inflammatory drug. Furthermore, it is lipophilic with the molecular size suitable for inclusion within the pores of $CaCO_3$ microparticles. The porous inorganic particles will enhance the drug loading with the capillary force of the nanopores and the polyelectrolyte multilayer shells will reduce the release rate and assuage the initial burst release. Similar combination of polyelectrolyte multilayer films formed with the LbL assembly and the core of porous $CaCO_3$ microparticles has been reported for the different purpose of fabricating microcapsules by removing the sacrificial $CaCO_3$ core after deposition (Volodkin et al., 2004a,b; Sukhorukov et al., 2004).

## 2. Materials and methods

### 2.1. Materials

Sodium poly(styrene sulfonate) (PSS, Aldrich, MW 70,000), protamine sulfate (PRO, Sigma), ibuprofen (Juhua Group Corporation Pharmaceutical Factory, China), $CaCl_2{\cdot}H_2O$ and $Na_2CO_3$ (Guangzhou Chemical Factory, China) were used without further purification. Highly purified water was obtained by deionization and filtration with a Millipore purification apparatus (resistivity higher than 18.2 MΩ cm). Other chemicals were all analytical reagents and used as received.

### 2.2. Preparation of porous $CaCO_3$ microparticles

Porous $CaCO_3$ microparticles were prepared by rapid mixing of equal volume of $CaCl_2$ and $Na_2CO_3$ aqueous solutions. Typically, 0.2 M $CaCl_2$ was rapidly poured into an equal volume of 0.2 M $Na_2CO_3$ solution (containing 4 g/L PSS) at room temperature. After vigorous agitation with a magnetic stirrer, the precipitate was filtered off, thoroughly washed with pure water, and dried in air. The course of the reaction was observed with a light microscope. The simple procedure results in highly homogeneous spherical porous $CaCO_3$ microparticles with an average diameter of 5 μm.

### 2.3. Drug loading

Before loading, $CaCO_3$ microparticles were washed with acetone and dried in a vacuum oven at 50 °C. 0.2 g of dried $CaCO_3$ microparticles were soaked in 5 mL IBU solution of 50 mg/mL in a closed batch to prevent evaporation of the liquid. Five solvents of dimethylsulfoxide (DMSO), dimethylformamide (DMF), dimethylacetamide (DMA), ethanol and hexane were used for loading. Afterward, the suspension was brought to equilibrium under gentle stirring for 24 h. Longer loading time did not increase the amount of IBU incorporated. Subsequently, the IBU-loaded $CaCO_3$ microparticles were collected by centrifugation, washed with ethanol to remove the adsorbed IBU on the external surface, and dried in a vacuum oven at 50 °C to completely evaporate

the solvents from the impregnated materials. Repeating the loading process, we obtained the $CaCO_3$ microparticles with different adsorbed amounts of IBU. The IBU-loaded $CaCO_3$ microparticles were ground into powder and loaded IBU was extracted from the powder by ethanol for 24 h. After centrifugation, the IBU concentration in the supernatant was determined with ultraviolet (UV) absorbance at 222 nm (Qiu et al., 2001) measured by a Hitachi U-3010 UV–vis photometer with the help of calibration curve describing the absorbance–concentration relationship. The amount of incorporated IBU $\Gamma$ expressed as milligram IBU/g $CaCO_3$ was evaluated. Thermogravimetric analysis (TGA) was also used to determine the amount of loaded IBU from the weight loss at the temperature corresponding to the loaded IBU thermodecomposition.

### 2.4. Encapsulation by polyelectrolyte multilayers

Polycation PRO and polyanion PSS were deposited on the IBU-loaded $CaCO_3$ microcapsules with the LbL self-assembly in water. To prevent the loaded IBU from dissolving during the LbL process, polyelectrolyte solutions and rinsing water were saturated with IBU. The first layer was formed by the addition of 5 mL of 2 mg/mL aqueous PRO solution containing 0.5 M NaCl into 0.02 g of the IBU-loaded $CaCO_3$ microparticles. The mixture was incubated for 15 min under gentle shaking. The excess polyelectrolyte was removed by three repeated refine circles of centrifugation (4000 rpm, 4 min)/washing/redispersion in water. The following PSS layer was deposited using the same procedure with 5 mL of 2 mg/mL PSS solution with 0.5 M NaCl. Subsequently, alternating PRO and PSS layers were deposited in the identical way until the desired layer number was achieved. These encapsulated IBU-loaded microparticles were collected by centrifugation, rinsed with pure water and then dried in a vacuum oven prior to the release experiment to remove the IBU adsorbed on the surface.

### 2.5. In vitro release

Dried pure IBU microcrystals (2.5 mg), the IBU-loaded $CaCO_3$ microparticles (30 mg, $\Gamma$ = 64.1 mg/g from TGA, ca. 1.8 mg IBU) and the encapsulated IBU-loaded microparticles (30 mg, ca. 1.8 mg IBU) were put in dialysis bags (cut-off MW 8000) with 10 mL release medium separately and then immersed in 390 mL release medium. The in vitro release was performed with continuously stirring at 37 °C. Two different pH solutions were used as the release medium as pH 1.2 solution (a simulated gastric fluid, prepared by diluting a concentrated HCl solution) and pH 7.4 solution (a simulated intestinal fluid, prepared with 0.02 M phosphate buffer). Because the saturation solubility of ibuprofen in pH 1.2 and pH 7.4 buffer solutions is 0.036 and 6.14 mg/mL (Qiu et al., 2001), respectively, the IBU concentration in each release solution was far from saturation. Three millilitre solution was withdrawn from the release medium at certain time intervals and the IBU concentration was determined with UV absorbance. The solution was then returned after measurement.

### 2.6. Characterization

For scanning electron microscopy (SEM), observation with a Philips XL 30 at the acceleration voltage of 15 kV, samples were prepared by dropping the particle suspension on a glass slide, dried overnight, then sputtered with gold.

The specific surface area, porous volume and porous size distribution of $CaCO_3$ microparticles were determined following the Brunauer–Emmett–Teller (BET) method of nitrogen adsorption/desorption at −196 °C with an ASAP2010 surface area analyzer (Micromeritics Instrument, USA).

Infrared (IR) spectra were measured with a Bruker Vector 33 on carefully dried samples embedded in KBr pellets. IBU-loaded microparticles were ground to powder before measurement.

Thermogravimetric analysis curves of the samples were collected with a thermoanalyzer (TG 209, NETZCH Co.) within a temperature range of 24–900 °C and with the rate of increasing temperature of 10 °C/min.

$\zeta$-Potential of each adsorbing layer on the IBU-loaded microparticles dispersed in pure water was determined with a Brookhaven zeta-potential analyzer and the $\zeta$-potential value was the average of three successive measurements.

Powder X-ray patterns were recorded using a Rigaku D/max-3A instrument (monochromated Cu K$\alpha$ radiation). Typically, the diffractogram was recorded in a $2\theta$ range of 5–25°C.

## 3. Results and discussion

### 3.1. Preparation of porous $CaCO_3$ microparticles

Preparation of $CaCO_3$ nano and microparticles has been a subject of many studies due to its great importance in biotechnology, medicine, materials science, as well as its wide applications in industry and many other fields. Fig. 2 displays SEM photos of different magnifications for our $CaCO_3$ microparticles prepared with a simple and reproducible procedure. Uniform and spherical $CaCO_3$ microparticles with a rather narrow size distribution from 4 to 6 μm can be observed from Fig. 2a. Their surface morphology presented in Fig. 2b and c looks very rough with a great number of carbonate nanoparticles on it. Abundant channel pores with size about 20 nm can be seen in the $CaCO_3$ microparticles from Fig. 2c.

PSS plays a very important role in the preparation. The $CaCO_3$ microparticles would have a broad size distribution and aggregation if there were no PSS added. Usually, the spherical $CaCO_3$ microparticle will turn to rhombohedral calcite microcrystal after several weeks of storage in water at room temperature because of recrystallization (Volodkin et al., 2004a,b). While the microparticles prepared with PSS have no obvious shape change during 6 months of storage in water. Negatively charged PSS is adsorbed on the surface of carbonate nanoparticles constituting the porous $CaCO_3$ microparticles and prevents the recrystallization. Volodkin et al. found that more than 80% of just-prepared porous $CaCO_3$ microparticles without dispersants recrystallized after storage overnight in water (Volodkin et al., 2004a). The morphology of the microcrystals formed after recrystallization was similar to that of usual $CaCO_3$ microcrys-

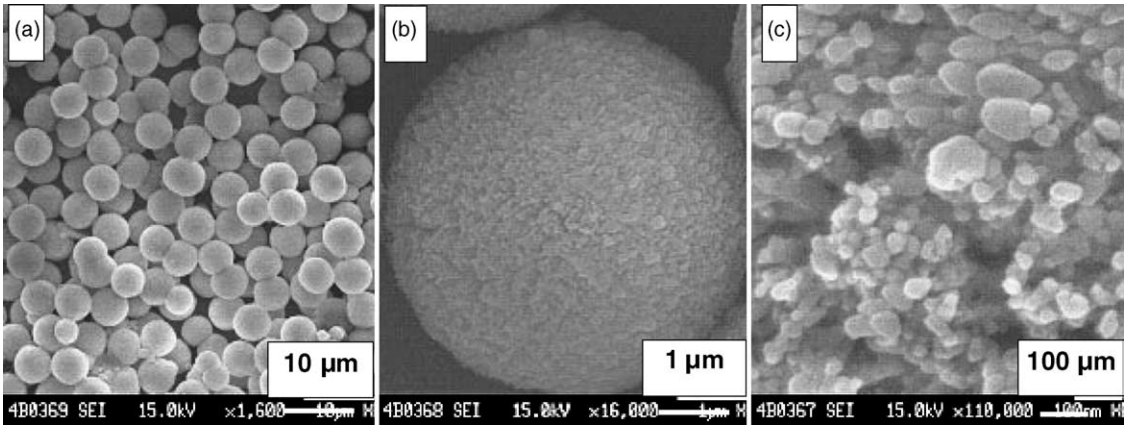


Fig. 2. SEM photos of different magnifications for $CaCO_3$ microparticles: (a) overview, (b) single particle and (c) enlarged part of a particle.

tals. When the microparticles were dispersed in the solution of polyelectrolytes (PSS, PAH) or proteins, less than 10–20% of the microparticles changed into microcrystals after overnight storage. High stability of the $CaCO_3$ microparticles in water is very important for the following LbL self-assembly.

### 3.2. IBU loading

Adsorption of IBU into the porous $CaCO_3$ microparticles was performed in the solvents of different polarities. IBU can be adsorbed from all these five solvents and the amount of one-time adsorption $\Gamma$ determined by UV is summarized in Table 1. $\Gamma$ increases with the decrease in the solvent polarity expressed by the dielectric constant $\varepsilon$ with an exception of the adsorption from DMSO. Although $\Gamma$ from hexane was attractive, we did not select hexane as the solvent in the following experiments owing to the toxicity of possibly residual hexane for the pharmaceutical usage. Ethanol was chosen as the adsorption solvent in the following work because of its reasonable $\Gamma$ value of 45.1 mg/g, convenience and non-toxicity. Charnay et al. (2004) also reported the solvent polarity effect on the IBU loading with mesoporous MCM 41 and found the highest $\Gamma$ value of 590 mg/g from hexane. The surface affinity of porous materials has significant effects on the adsorption capability to the drug (Otsuka et al., 2000). However, the effect of adsorbed PSS on IBU loading has not been investigated in this work because stable and porous $CaCO_3$ microparticles cannot be fabricated without adding PSS, which should be used as reference.

The IR spectra of the $CaCO_3$ microparticles, free IBU and IBU-loaded $CaCO_3$ microparticles are shown in Fig. 3. The IR spectrum of the IBU-loaded $CaCO_3$ microparticles reflects the characteristic absorption bands of IBU and calcium carbonate without obvious new bands, which indicates that IBU adsorption in $CaCO_3$ is of physical. Fig. 4 depicts TGA curves for the $CaCO_3$ microparticles, free IBU, and IBU-loaded $CaCO_3$ microparticles loaded one and three-times from IBU ethanol solution. The $CaCO_3$ microparticles started to lose weight at 700 °C and lost about 40% weight at 750 °C. Free IBU started to lose weight at 120 °C and lost its weight completely at 230 °C. The loaded IBU started to lose weight at 420 °C, 300 °C higher than that of free IBU. The $\Gamma$ evaluated from the TGA curve *c* for the one-time loading is 33.9 mg/g, lower than 45.1 mg/g determined by UV absorbance. The reason seems to be that most adsorbed IBU stays in the pores and not at the external surface enhancing the resistance to the thermo-decomposition and that the decomposed IBU residues remain in the pore inner of the porous $CaCO_3$ microparticles and cannot completely escape

Table 1
Adsorption of IBU into porous $CaCO_3$ microparticles from different solvents

| Solvent | $\varepsilon$ (25 °C) | $\Gamma$ (mg/g) |
|---|---|---|
| Dimethylsulfoxide | 46.7 | 37.6 |
| Dimethylformamide | 37.8 | 29.3 |
| Dimethylacetamide | 37.8 | 37.7 |
| Ethanol | 24.5 | 45.1 |
| Hexane | 1.88 | 87.3 |

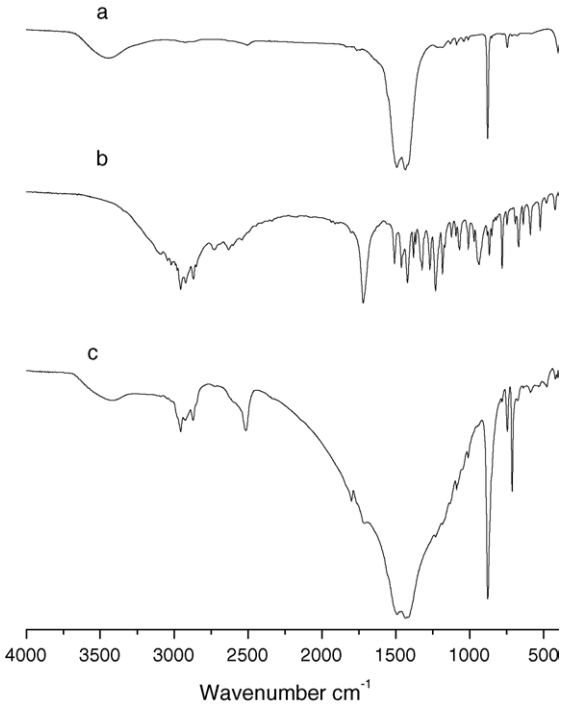


Fig. 3. IR spectra of (a) $CaCO_3$ microparticle, (b) IBU microcrystal and (c) IBU-loaded $CaCO_3$ microparticle.

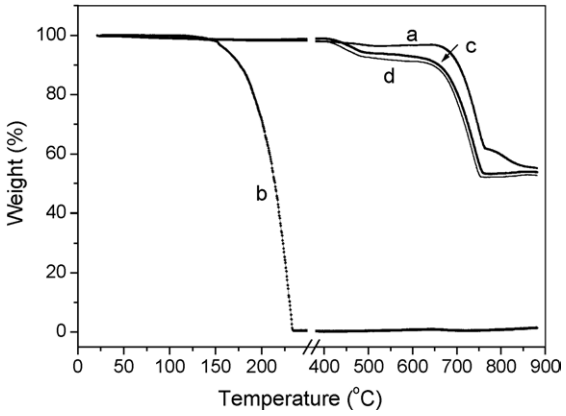


Fig. 4. TGA curves of (a) $CaCO_3$ microparticle, (b) IBU microcrystal and $CaCO_3$ microparticles after IBU loading one time (c) and three-times (d).

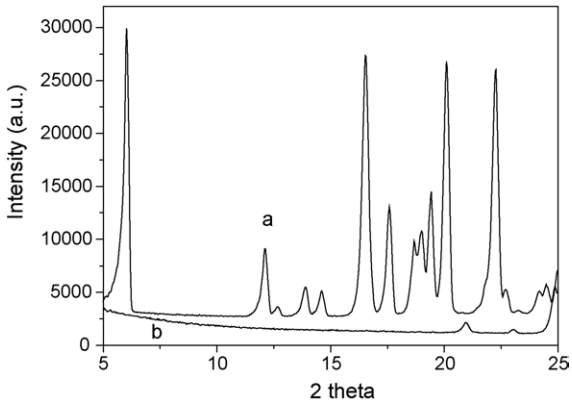


Fig. 6. XRD pattern of (a) IBU microcrystal and (b) IBU-loaded $CaCO_3$ microparticle.

Table 2
Characteristics of porous $CaCO_3$ microparticles before and after IBU loading

| | $S_{BET}$ ($m^2$/g) | $V_{mes}$ ($cm^3$/g) |
|---|---|---|
| Before loading | 40.02 | 0.23 |
| After loading | 24.44 | 0.17 |

easily. The $\Gamma$ evaluated from the TGA curve *d* for the three-time loading is 64.1 mg/g, indicating the adsorbed amount increased with multiple loading processes.

BET analysis was carried out in order to determine the change in specific surface area, pore volume, and pore size distribution of the porous $CaCO_3$ microparticles before and after loading IBU three-times and the results are shown in Table 2 and Fig. 5. The density of calcium carbonate is 2.7 g/$cm^3$, so the surface area of solid spherical particles with a diameter of 5 μm is only 0.44 $m^2$/g. The surface area $S_{BET}$ of present $CaCO_3$ microparticles is 40.02 $m^2$/g, about 100 times of the solid $CaCO_3$ particles. The pore volume $V_{mes}$ is 0.23 $cm^3$/g and the specific volume of solid $CaCO_3$ calculated from its density is 0.37 $cm^3$/g. Therefore, the pore in the porous $CaCO_3$ microparticle takes about 38.3% of the total particle volume. After loading IBU, the surface area $S_{BET}$ decreases to 24.44 $m^2$/g and the pore volume $V_{mes}$ is reduced to 0.17 $cm^3$/g as known from Table 2. The $\Gamma$ value for three-time loading is estimated as ∼51 mg/g from the decrease in pore volume and density of IBU (assumed as 1 g/$cm^3$), which is smaller than 64.1 mg/g estimated from the TGA data.

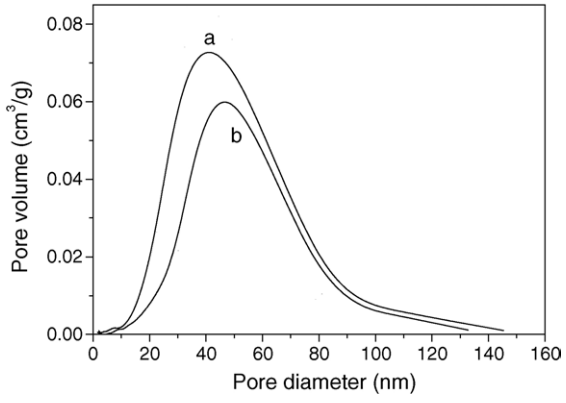


Fig. 5. Pore size distribution of $CaCO_3$ microparticles before (a) and after (b) IBU loading.

The pore size distribution of the $CaCO_3$ microparticles before and after IBU loading is presented in Fig. 5. The volume of small pores decreases more than that of large ones after IBU loading. This is due to the high surface free energy and easy being filled of the smaller pores. Therefore, when the $CaCO_3$ microparticles were immersed in IBU solution, the IBU will be preferentially adsorbed into the smaller pores.

The surface area $S_{BET}$ of $CaCO_3$ microparticles prepared by Volodkin et al. (2004a,b) without adding any dispersants was 8.8 $m^2$/g, much smaller than that of our $CaCO_3$ microparticles of 40.02 $m^2$/g. The dispersant PSS has an important contribution to the large $S_{BET}$ due to the loose packing of the as-formed crystal carbonate with PSS absorption.

The X-ray diffraction of pure IBU and the IBU-loaded $CaCO_3$ microparticles is plotted in Fig. 6. There is not any diffraction peak for the loaded IBU appearing at low 2$\theta$ and the diffraction of calcium carbonate does not exist in this 2$\theta$ range. Thus, the present result means that IBU adsorbed in the $CaCO_3$ pore channels is in the amorphous state without crystallization, otherwise the diffraction peaks of IBU crystals should be observed (Charnay et al., 2004). This is in agreement with the consideration of crystallization within a confined space, which has shown that the crystallization can occur only when the pore size is much larger than the molecule size, e.g., about 20 times of the molecule length (Sliwinska-Bartkowiak et al., 2001). This becomes another evidence that most adsorbed IBU stays in the pore inner and not at the external surface.

### 3.3. Encapsulation of IBU adsorbed $CaCO_3$ microparticles

In order to reduce the release rate and to assuage the initial burst, PRO and PSS were alternately deposited on the IBU-loaded $CaCO_3$ microparticles via the LbL self-assembly. This encapsulation process was followed by the ζ-potential shown in Fig. 7a. The ζ-potential is −16.7 mV for the bare IBU-loaded $CaCO_3$ microparticles, and then changes into 17.5 mV for the first PRO layer and −37.2 mV for the first PSS layer. The obvious switching of ζ-potential indicates successful alternating deposi-

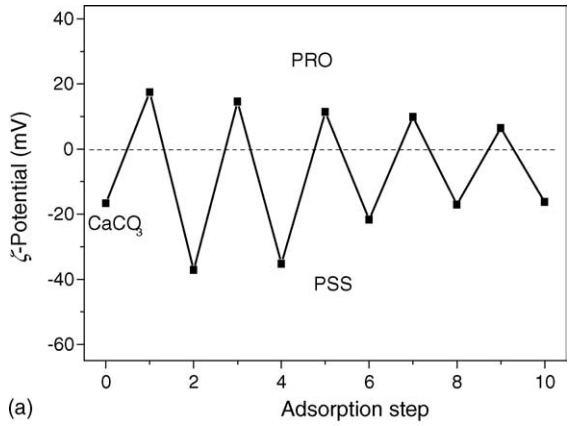


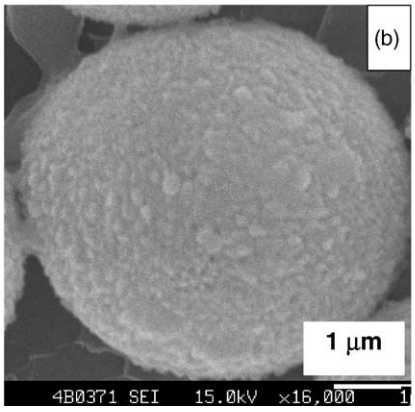


Fig. 7. (a) $\zeta$-Potential as a function of adsorption step for PRO and PSS deposited on the IBU-loaded $CaCO_3$ microparticles; (b) SEM image of the IBU-loaded microcapsules coated with five bilayers of PRO/PSS.

tion of the polycation PRO and polyanion PSS directly on the IBU-loaded $CaCO_3$ microparticles and the IBU-loaded microcapsules were encapsulated. SEM image of the IBU-loaded microcapsules encapsulated with five bilayers of PRO/PSS is presented in Fig. 7b. The surface of the microcapsules looks somewhat smooth and slight conglutination occurs among them. This is owing to the bridging of oppositely charged PRO and PSS chains adsorbed on the neighboring particles.

### 3.4. In vitro drug release

The IBU released from the particles was monitored with UV absorbance of the release medium and Fig. 8 depicts the release profiles of the IBU crystals, IBU-loaded $CaCO_3$ microparticles and encapsulated IBU-loaded $CaCO_3$ microparticles in the simulated gastric fluid (pH 1.2) at 37 °C. The half release time $t_{1/2}$ in this medium is 180, 70 and 100 min for the IBU crystals, IBU-loaded $CaCO_3$ microparticles and IBU-loaded microcapsules, respectively. The total release time for the corresponding particles is 500, 250 and 500 min. The IBU crystal shows the slowest release rate because its solubility in acidic solution is very low (saturation solubility at pH 1.2 is 0.036 mg/mL) and large aggregation of IBU crystals forms in the dialysis bag. The IBU in porous $CaCO_3$ microparticles is amorphous (Fig. 6) and is adsorbed on the pore surface as a very thin film, which results in a rapid dissolution and then a rapid release. As

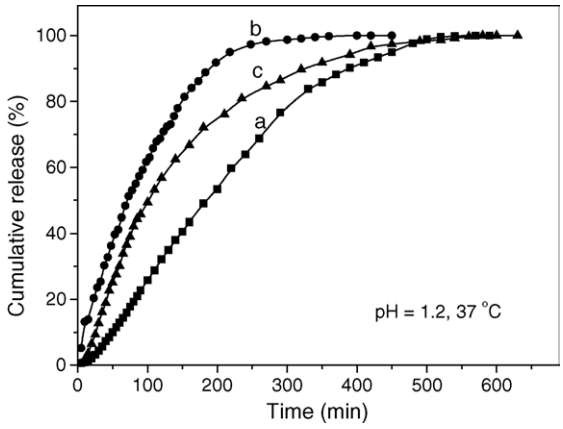


Fig. 8. Release profiles of (a) bare IBU microcrystals, (b) IBU-loaded $CaCO_3$ microparticles and (c) IBU-loaded microcapsules with five bilayers of PRO/PSS in simulated gastric fluid (pH 1.2) at 37 °C.

expected, the IBU-loaded microcapsules, i.e., the IBU-loaded $CaCO_3$ microparticles covered with five bilayers of PRO/PSS have a considerable slow release rate for the polyelectrolyte multilayers on the particles obstruct the diffusion of loaded IBU into the solution.

The release profiles of the particles in the simulated intestinal fluid (pH 7.4) at 37 °C are shown in Fig. 9. In this medium, the half release time $t_{1/2}$ is 12, 25 and 60 min for the IBU crystals, IBU-loaded $CaCO_3$ microparticles and IBU-loaded microcapsules, respectively, and the corresponding total release time is 150, 230 and 320 min. The release is much faster in this simulated intestinal fluid because the IBU saturation solubility at pH 7.4 is 6.14 mg/mL, much higher than that in the simulated gastric fluid (pH 1.2). What is important is that the initial release burst has been assuaged and the release rate has been slowed down with covering the polyelectrolyte multilayers on the IBU-loaded $CaCO_3$ microparticles.

Furthermore, the in vitro release was performed successively in two simulated fluids: in the gastric fluid for 30 min and then in the intestinal fluid for rest of the time in order to imitate the process of oral administration (Fig. 10). The IBU-loaded

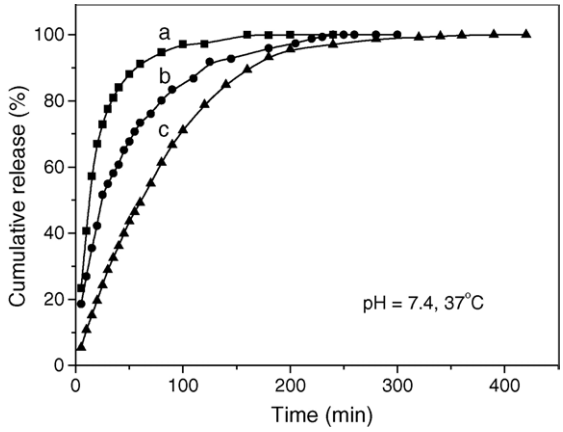


Fig. 9. Release profiles of (a) bare IBU microcrystals, (b) IBU-loaded $CaCO_3$ microparticles and (c) IBU-loaded microcapsules with five bilayers of PRO/PSS in simulated intestinal fluid (pH 7.4) at 37 °C.

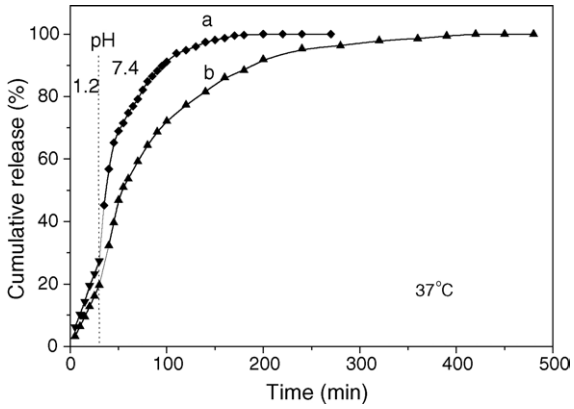


Fig. 10. Release profiles of (a) IBU-loaded $CaCO_3$ microparticles and (b) IBU-loaded microcapsules with five bilayers of PRO/PSS in simulated gastric fluid for the first 30 min and then in simulated intestinal fluid for rest of the time at 37 °C.

microcapsules display a slower release rate than that of the IBU-loaded $CaCO_3$ microparticles as 27.3% and 19.6% of IBU are lost in the gastric fluid for the IBU-loaded $CaCO_3$ microparticles and IBU-loaded microcapsules, respectively. The total release time for the corresponding particles is 220 and 420 min.

The in vitro drug release investigation found that the LbL deposited polyelectrolyte multilayer is very efficient to reduce the release rate and assuage the initial burst for drugs loaded in porous inorganic microparticles. This approach to fabricating polymer/inorganic hybrid core-shell microcapsules loading functional substances in the pores of inorganic cores demonstrates great promise for many biomedical and biotechnological applications, especially drug sustained release.

## Acknowledgments

The financial support to this work of the NSF of China (no: 90206010, 20574023, 20534020), the NSF of Guangdong province (no: 031380), and the Scientific and Technologic Program of Guangzhou municipal (no: 2003Z3-D2031) is gratefully acknowledged.

## References

Ai, H., Jones, S., de Villiers, M., Lvov, Y.M., 2003. Nano-encapsulation of furosemide microcrystals for controlled drug release. J. Control. Release 86, 59–68.

Allen, T.M., Cullis, P.R., 2004. Drug delivery systems: entering the mainstream. Science 303, 1818–1822.

An, Z.H., Lu, G., Möhwald, H., Li, J.B., 2004. Self-assembly of human serum albumin (HSA) and L-α-dimyristoylphosphatidic acid (DMPA) microcapsules for controlled drug release. Chem. Eur. J. 10, 5848–5852.

Benita, S. (Ed.), 1996. Microencapsulation, Drugs and the Pharmaceutical Science. Marcel Dekker, New York.

Brigger, I., Dubernet, C., Couvreur, P., 2002. Nanoparticles in cancer therapy and diagnosis. Adv. Drug Deliv. Rev. 54, 631–651.

Caruso, F., 2001. Nanoengineering of particle surfaces. Adv. Mater. 13, 11–22.

Caruso, F., Möhwald, H., 1999. Protein multilayer formation on colloids through a stepwise self-assembly technique. J. Am. Chem. Soc. 121, 6039–6046.

Charnay, C., Begu, S., Tourne-Peteilh, C., Nicole, L., Lerner, D.A., Devoisselle, J.M., 2004. Inclusion of ibuprofen in mesoporous templated silica: drug loading and release property. Eur. J. Pharm. Biopharm. 57, 533–540.

Dai, Z.F., Heilig, A., Zastrow, H., Donath, E., Möhwald, H., 2004. Novel formulations of vitamins and insulin by nanoengineering of polyelectrolyte multilayers around microcrystals. Chem. Eur. J. 10, 6369–6374.

Decher, G., Schlenoff, J.B. (Eds.), 2003. Multilayer Thin Films: Sequential Assembly of Nanocomposite Material. Wiley-VHC, Weinheim.

El-Ghannam, A., Ahmed, K., Omran, M., 2005. Nanoporous delivery system to treat osteomyelitis and regenerate bone: gentamicin release kinetics and bactericidal effect. J. Biomed. Mater. Res. B: Appl. Biomater. 73, 277–284.

Fisher, K.A., Huddersman, K.D., Taylor, M.J., 2003. Comparison of micro- and mesoporous inorganic materials in the uptake and release of the drug model fluorescein and its analogues. Chem. Eur. J. 9, 5873–5878.

He, C.Y., Liang, Z.P., Wang, C.Y., Liu, X.X., Tong, Z., 2005. Immobilization of superoxide dismutase by layer-by-layer assembly on surface of PS colloid particles and their bioactivity. Chem. J. Chin. U. (Chin.) 26, 88–92.

Kim, H.W., Knowles, J.C., Kim, H.E., 2004. Hydroxyapatite/poly(epsilon–caprolactone) composite coatings on hydroxyapatite porous bone scaffold for drug delivery. Biomaterials 25, 1279–1287.

Kortesuo, P., Ahola, M., Kangas, M., Leino, T., Laakso, S., Vuorilehto, L., Yli-Urpo, A., Kiesvaara, J., Marvola, M., 2001. Alkyl-substituted silica gel as a carrier in the controlled release of dexmedetomidine. J. Control. Release 76, 227–238.

Li, Z.Z., Wen, L.X., Shao, L., Chen, J.F., 2004. Fabrication of porous hollow silica nanoparticles and their applications in drug release control. J. Control. Release 98, 245–254.

Liang, Z.P., Wang, C.Y., Sun, Q.L., Tong, Z., 2004. Novel microcapsule fabricated by LbL nano self-assembly. Prog. Chem. 16, 485–491.

Liang, Z.P., Wang, C.Y., Tong, Z., Ye, W.H., Ye, S.Q., 2005. Bio-catalytic nanoparticles with urease immobilized in multilayer assembled through layer-by-layer technique. React. Funct. Polym. 63, 85–94.

Mao, Z.W., Ma, L., Gao, C.Y., Shen, J.C., 2005. Preformed microcapsules for loading and sustained release of ciprofloxacin hydrochloride. J. Control. Release 104, 193–202.

Otsuka, M., Tokumitsu, K., Matsuda, Y., 2000. Solid dosage form preparations from oily medicines and their drug release. Effect of degree of surface-modification of silica gel on the drug release from phytonadione-loaded silica gels. J. Control. Release 67, 369–384.

Pargaonkar, N., Lvov, L.M., Li, N., Steenekamp, J.H., de Villiers, M.M., 2005. Controlled release of dexamethasone from microcapsules reduced by polyelectrolyte layer-by-layer nanoassembly. Pharm. Res. 22, 826–835.

Peyratout, C.S., Dahne, L., 2004. Tailor-made polyelectrolyte microcapsules: from multilayers to smart containers. Angew. Chem. Int. Ed. 43, 3762–3783.

Qiu, X., Leporatti, S., Donath, E., Möhwald, H., 2001. Studies on the drug release properties of polysaccharide multilayers encapsulated ibuprofen microparticles. Langmuir 17, 5375–5380.

Schuler, C., Caruso, F., 2000. Preparation of enzyme multilayers on colloids for biocatalysis. Macromol. Rapid Commun. 21, 750–753.

Sliwinska-Bartkowiak, M., Dudziak, G., Gras, R., Sikorski, R., Radhakrishnan, R., Gubbins, K.E., 2001. Freezing behavior in porous glasses and MCM-41. Colloid Surf. A 187–188, 523–529.

Sukhorukov, G.B., Volodkin, D.V., Gunther, A.M., Petrov, A.I., Shenoy, D.B., Möhwald, H., 2004. Porous calcium carbonate microparticles as templates for encapsulation of bioactive compounds. J. Mater. Chem. 14, 2073–2081.

Sun, Q.L., Tong, Z., Wang, C.Y., Ren, B.Y., Liu, X.X., Zeng, F., 2005. Charge density threshold for LbL self-assembly and small molecule diffusion in polyelectrolyte multilayer films. Polymer 46, 4958–4966.

Suzuki, K., Yumura, T., Tanaka, Y., Akashi, M., 2001. Thermo-responsive release from interpenetrating porous silica–poly(*N*-isopropylacrylamide) hybrid gels. J. Control. Release 75, 183–189.

Tiourina, O.P., Sukhorukov, G.B., 2002. Multilayer alginate/protamine micro-sized capsules: encapsulation of α-chymotrypsin and controlled release study. Int. J. Pharm. 242, 155–161.

Torchilin, V.P., 2005. Recent advances with liposomes as pharmaceutical carriers. Nat. Rev. Drug Discov. 4, 145–160.

Volodkin, D.V., Larionova, N.I., Sukhorukov, G.B., 2004a. Protein encapsulation via porous $CaCO_3$ microparticles templating. Biomacromolecules 5, 962–972.

Volodkin, D.V., Petrov, A.I., Prevt, M., Sukhorukov, G.B., 2004b. Matrix polyelectrolyte microcapsules: new system for macromolecule encapsulation. Langmuir 20, 3398–3406.

Ye, S.Q., Wang, C.Y., Liu, X.X., Tong, Z., 2005a. Deposition temperature effect on release rate of indomethacin microcrystals from microcapsules of layer-by-layer assembled chitosan and alginate multilayer films. J. Control. Release 106, 319–328.

Ye, S.Q., Wang, C.Y., Liu, X.X., Tong, Z., 2005b. Multilayer nanocapsules of polysaccharide chitosan and alginate through layer-by-layer assembly directly on PS nanoparticles for release. J. Biomater. Sci. Polym. Ed. 16, 909–924.

Zahr, A.S., de Villiers, M., Pishko, M.V., 2005. Encapsulation of drug nanoparticles in self-assembled macromolecular nanoshells. Langmuir 21, 403–410.